**Climate
of the Past**

Estimating 750 years of temperature variations and uncertainties in the Pyrenees by tree-ring reconstructions and climate simulations

I. Dorado Liñán[1,2], U. Büntgen[3], F. González-Rouco[4], E. Zorita[5,6], J. P. Montávez[7], J. J. Gómez-Navarro[7], M. Brunet[8], I. Heinrich[1], G. Helle[1], and E. Gutiérrez[2]

[1]Helmholtz Centre Potsdam, German Centre for Geosciences, Climate Dynamics and Landscape Evolution, Potsdam, Germany
[2]Universitat de Barcelona, Departament d'Ecologia, Barcelona, Spain
[3]Swiss Federal Research Institute WSL, 8903 Birmensdorf, Switzerland
[4]Universidad Complutense de Madrid, Ciudad Universitaria, 28040 Madrid, Spain
[5]Helmholtz-Zentrum-Geesthacht, Geesthacht, Germany
[6]Bert Bolin Centre for Climate Research, Stockholm University, Sweden
[7]Departamento de Física, Universidad de Murcia, Murcia, Spain
[8]Centre for Climate Change, Universitat Rovira i Virgili, Tarragona, Spain

Correspondence to: I. Dorado Liñán (isabel@gfz-potsdam.de)

Abstract. Past temperature variations are usually inferred from proxy data or estimated using general circulation models. Comparisons between climate estimations derived from proxy records and from model simulations help to better understand mechanisms driving climate variations, and also offer the possibility to identify deficiencies in both approaches.

This paper presents regional temperature reconstructions based on tree-ring maximum density series in the Pyrenees, and compares them with the output of global simulations for this region and with regional climate model simulations conducted for the target region. An ensemble of 24 reconstructions of May-to-September regional mean temperature was derived from 22 maximum density tree-ring site chronologies distributed over the larger Pyrenees area. Four different tree-ring series standardization procedures were applied, combining two detrending methods: 300-yr spline and the regional curve standardization (RCS). Additionally, different methodological variants for the regional chronology were generated by using three different aggregation methods. Calibration verification trials were performed in split periods and using two methods: regression and a simple variance matching. The resulting set of temperature reconstructions was compared with climate simulations performed with global (ECHO-G) and regional (MM5) climate models.

The 24 variants of May-to-September temperature reconstructions reveal a generally coherent pattern of inter-annual to multi-centennial temperature variations in the Pyrenees region for the last 750 yr. However, some reconstructions display a marked positive trend for the entire length of the reconstruction, pointing out that the application of the RCS method to a suboptimal set of samples may lead to unreliable results.

Climate model simulations agree with the tree-ring based reconstructions at multi-decadal time scales, suggesting solar variability and volcanism as the main factors controlling preindustrial mean temperature variations in the Pyrenees. Nevertheless, the comparison also highlights differences with the reconstructions, mainly in the amplitude of past temperature variations and in the 20th century trends. Neither proxy-based reconstructions nor model simulations are able to perfectly track the temperature variations of the instrumental record, suggesting that both approximations still need further improvements.

1   Introduction

Estimations of future climate change indicate that variations at regional scales may be larger than the global average (IPCC, 2007). However, these regional projections are hampered by the limited knowledge of the mechanisms that give rise to variability at multi-decadal and longer time scales. One reason is the short length of the available instrumental records. The relative abundance of proxy records during the last millennium (e.g. Jones et al., 2009) offers the possibility to reconstruct climate parameters such as temperature and precipitation, improving our understanding of past regional climate variability at interdecadal and longer time scales (Jansen et al., 2007). Currently, two main approaches are being used to advance this line of research: (1) creating new or extending the existing climate reconstructions back in time using documentary evidence or environmental proxies such as tree-ring parameters (width, density, isotopic content), corals, speleothems (Jones et al., 2009); and (2) simulations of natural and forced climate variability using climate models (e.g. Zorita et al., 2005; González-Rouco et al., 2009; Junglcaus et al., 2010).

Tree-rings may contain useful information on past environmental conditions, which can be used to reconstruct past climate using statistical relationships to a target climate variable (Fritts, 1976; Cook and Kairiukstis, 1990). In this respect, tree-ring width and density are the most widely used proxies for the last millennium, and their links to seasonal temperatures have been extensively studied (Briffa et al., 2002, 2004; Büntgen et al., 2006, 2007, 2008; Esper et al., 2002, 2005a; Grudd, 2008). Although tree-ring measurements are accurately annually dated, their ability to encode centennial to multi-centennial climate variability is often limited by the standardization technique used to remove age-related trends. The climate signal at these time scales may be distorted by the technique used to remove non-climatic variations in tree-ring series (Cook et al., 1995; Esper et al., 2002, 2003; Briffa and Melvin, 2008). In addition to the standardization issue, it is desirable that the climate reconstructions based on proxies represent a climate signal that is not locally confined. This is necessary in order to bridge the gap in the spatial scale between the coarse resolution of climate models and the local proxy-based climate reconstructions. Thus, individual or site chronologies are ideally aggregated into one regional chronology that captures a regional climate signal, the same spatial resolution that climate models are intended to represent. Furthermore, the technique applied to transform tree-ring parameters to meteorological units also implies a challenge: whereas simple linear regression methods may underestimate low-frequency variability, variance matching, in the following referred to as scaling, shows better performance in retaining large-scale variations but at the expense of inflated error estimates (Esper et al., 2005b; Zorita et al., 2010; McCarrol et al., 2011).

A variety of climate models of increasing complexity is available for palaeoclimate simulation experiments: from energy balance models (EBM; e.g. Hegerl et al., 2006) to three-dimensional coupled ocean-atmosphere general circulation models (GCMs; e.g. Zorita et al., 2005). GCMs have a global coverage, although their spatial resolution is still limited by computing power requirements. Additionally, the output of climate models is burdened by an important amount of uncertainty arising from limitations in the models themselves, as well as from the prescribed external forcings used to drive the simulations, which are mostly estimated from proxy data (Jansen et al., 2007). Thus, the validation of the models is necessary prior to using their simulated outputs. This validation is based on the assessment of their skill to reproduce the general circulation and main climatic features of the current observed climate, although this does not guarantee their reliability to project future or past climate changes.

The model ECHO-G was part of the Climate Model Intercomparison Project CMIP3, which was widely used in the Fourth Assessment Report of the Intergovernmental Panel on Climate Change (IPCC). The ECHO-G model was identified as one of the best performing models in the suite when benchmarked against recent temperature, precipitation and sea level pressure data (Gleckler et al., 2008). Alternatively, regional climate models (RCM) simulate a limited area, thus reducing the computational requirements and allowing simulations at higher spatial resolutions. Simulations with this kind of model over the last millennium have recently become available for specific regions (e.g. Gómez-Navarro et al., 2011, 2012). The development of RCM palaeoclimate simulations depends on the existence of GCM runs where boundary conditions are taken from. However, the higher RCM resolution improves several aspects of the climate simulation with coarser GCMs, such as a better representation of the interactions between the large-scale circulation and the orography, which plays an important role in regional climates. Additionally, the RCM employed here implements a set of physical parameterizations of the sub-grid processes that has been demonstrated to reproduce realistically the heterogeneous climate over the Iberian Peninsula (Gómez-Navarro et al., 2011). Thus, these model data allow in general for more realistic model-data comparisons.

Validations based on cross-comparisons between reconstructions and model estimates are still needed, especially at regional scales, since such comparisons offer the possibility to identify deficiencies in both approaches and thus to improve proxy-based reconstructions, climate models and forcing estimates (e.g. D'Arrigo et al., 1999; Collins et al., 2002; Tan et al., 2009; González-Rouco et al., 2009; Zorita et al., 2010; Gómez-Navarro et al., 2011).

In the climate context in the Iberian Peninsula, the Pyrenees range constitutes an interesting area for palaeoclimate reconstruction and simulations due to its location in the transition zones between the Eurosiberian and Mediterranean ecoclimatic regions, where future climate change is expected

to have large effects (IPCC, 2007). Furthermore, networks of tree-ring data suitable for developing temperature reconstructions (Büntgen et al., 2010) as well as global (González-Rouco et al., 2009) and regional (Gómez-Navarro et al., 2011, 2012) scale climate simulations are available for this region.

By using both proxy and model data, this work aims at two main objectives: (1) to generate an improved version of the tree-ring based reconstruction of past temperatures in the Pyrenees by using a larger dataset and evaluating the uncertainties related to the usage of several methodological variants; (2) to assess the realism of GCM and RCM simulations and their differences in reproducing available evidence of past climate variability over the Pyrenees area by comparing them to the tree-ring based climate reconstructions developed here.

With this purpose, in the first part of the study, we test different methods to develop the tree-ring based climate reconstructions, considering the most usual approaches for the standardization of the individual series, for the aggregation into a regional chronology and for the calibration-reconstruction technique applied. The resulting reconstruction variants are compared to a previously existing maximum temperature reconstruction based on tree-rings developed by Büntgen et al. (2008). In the second part, we compare the climate variability of the reconstruction based on the tree-ring records with that simulated by a GCM and a RCM over the Pyrenees area. We focus on identifying and discussing the possible causes for the different estimations of past climate changes.

2 Material and methods

A dataset of 804 individual maximum density (MXD) tree-ring series, grouped into 22 chronologies covering the Pyrenees area, was available for the present study. The network includes the two chronologies previously used to develop the first tree-ring based regional reconstruction of past maximum temperatures in the Pyrenees (Büntgen et al., 2008): additional data published in Büntgen et al. (2010), and a newly developed 700-yr long MXD chronology. Compared to the previous reconstruction of maximum temperature, the new dataset covers a wider area and uses a larger replication, not only in most recent centuries, but also in the earliest part of the period (1260–1350 AD).

The location, elevation and tree species at each site are indicated in Fig. 1. The species sampled were Mountain pine (*Pinus uncinata* Ramond ex DC. in Lam. et DC.), a shade-intolerant and long-lived conifer that grows under temperate subalpine climate conditions and dominates at elevations above 1800 m a.s.l., and Silver fir (*Abies alba* Mill.) that usually grows at humid sites on north facing, shady slopes and at elevations above 1200 m a.s.l. (Macias et al., 2006).

As described in Büntgen et al. (2008, 2010), to obtain the MXD measurements from tree-rings, all cores were sanded and visually cross-dated following dendrochronological procedures described by Stokes and Smiley (1968). The accuracies of the visual cross-dating and measurements were verified using the computer program COFECHA (Holmes, 1983). For the density measurements, lathes perpendicular to the wood fibres were extracted from 804 cores and analysed following X-ray microdensitometric techniques developed by Polge (1965). The output is a density profile of points taken at 0.01 mm intervals in the radial direction across each ring. The MXD along this direction was estimated for each year.

2.1 Site chronologies

In order to construct the MXD chronologies for each of the 22 sites, density series were processed according to standard dendrochronological techniques (Cook and Kairiukstis, 1990). The individual series were standardized to remove age trends in the mean by fitting a stiff function, which not only emphasizes inter-annual variations, but also preserves multi-decadal scale variations in the final chronology (Cook et al., 1995). To assess the uncertainty caused by the application of different standardizations, the individual series underwent different standardization procedures with ARSTAN (Cook and Holmes, 1986). Two detrending techniques were used to remove age trends: regional curve standardization (RCS; Esper et al., 2003) and a 300-yr cubic smoothing spline with a 50 % frequency response cut-off (300sp; e.g. Büntgen et al., 2010). In addition to these two detrending techniques, a power transformation (PT) for the stabilization of the variance in the individual series was alternately conducted (Cook and Peters, 1997). Although raw MXD series are often assumed to be homoscedastic, a conservative position was adopted, since the existence of long-term trends in the serial variance cannot be entirely rejected. Thus, a set of four different standardization procedures was applied considering the possible existence of trends in the variance: (1) RCS; (2) RCS preceded by PT (RCSPT); (3) 300sp; and (4) 300sp preceded by PT (300spPT). Finally, for each site, chronologies were constructed by using a bi-weight robust mean (Cook and Kairiukstis, 1990), which reduces the possible bias caused by extreme values. The final length of the chronologies was established by truncating the final chronologies when less than five contributing samples were available (Esper et al., 2003; Büntgen et al., 2008), leading to a maximum reliable time span of 1260–2005 AD (Fig. 2).

2.2 Regional Pyrenees chronologies

MXD individual series and site chronologies were standardized and aggregated into regional chronologies using three different approaches: (1) computing a simple arithmetic average of the 22 individual MXD chronologies (RCS_mean,
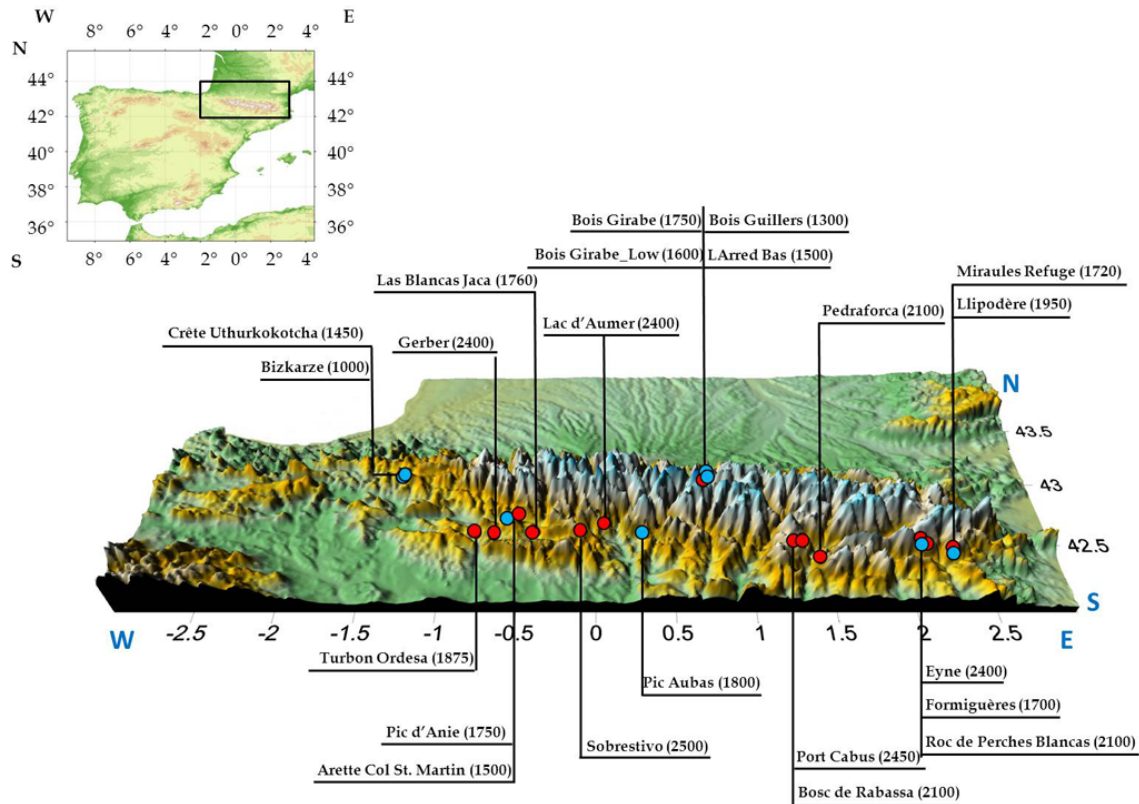
Fig. 1. Location of the 22 MXD chronologies. Red and blue circles indicate the tree species sampled at each site: *Pinus uncinata* and *Abies alba*, respectively. The elevations (in m a.s.l.) are indicated in brackets.

RCSPT_mean, 300sp_mean, 300spPT_mean); (2) computing a single chronology including all 804 individual series in one run (RCS_chrono, RCSPT_chrono, 300sp_chrono, 300spPT_chrono); and (3) conducting principal component analyses (Peters et al., 1981), computed separately for each time segment with a constant number of MXD chronologies to produce nested PCA regional chronologies (PCs_RCS; PCs_RCSPT; PCs_300sp; PCs_300spPT). The combination of the four different procedures for standardization and the three different procedures for aggregation yields a total of 12 different regional chronologies for the Pyrenees region.

Due to the different time spans covered by the 22 chronologies (Fig. 2), a total number of 25 PCA runs were performed for each of the four standardization methods (RCS, RCSPT, 300sp and 300spPT) in order to obtain the corresponding scores of the principal components (PCs) for each of the time segments. In addition, the spatial loadings, sometimes denoted as empirical orthogonal functions (EOFs), were also analyzed to assess the similarities and differences between their spatial patterns among the four standardization methods. For the EOF maps we use the loading that corresponds to the run5 (time span 1928–1977 AD), which includes all 22 MXD chronologies.

Simple correlations were used to assess the climate information contained in the regional chronologies. In mountainous regions such as the Pyrenees, temperature series have shown stronger inter-site relationships between distant sites than precipitation data, which display stronger variability at local spatial scales (Agusti-Panareda et al., 2000). Temperature is known to be the dominant climate factor controlling tree-growth at high-elevation sites in the Pyrenees (Macias et al., 2006; Büntgen et al., 2008, 2010). A regional record consisting of the data from six stations: Pamplona, San Sebastián, Zaragoza, Barcelona, Burgos and Huesca (Brunet et al., 2007, 2008) was available as a representative homogenized and high-quality temperature record of the area for the last 100 yr. All regional chronologies, together with the leading principal component PC1 of the PCA, were correlated with instrumental regional maximum, minimum and mean temperature from Brunet et al. (2007, 2008) at monthly and seasonal time scales (results not shown). May-to-September mean temperature (T_{MJJAS}) was identified as the most influencing parameter for tree growth.

2.3 Pyrenees reconstructions

Pyrenees temperature reconstructions were obtained using both scaling and regression methods (Esper et al., 2005b) applied to the different regional chronologies developed. Thus, from the collection of 12 regional MXD chronologies built
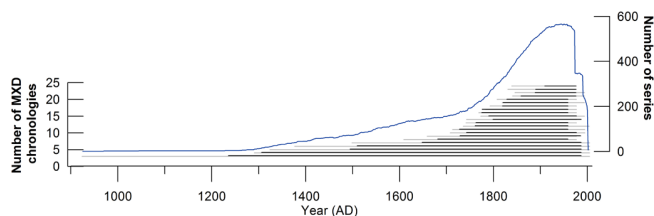
Fig. 2. Total time span (grey line) and reliable time span (black line) after truncation of the 22 MXD chronologies when less than five series were available. Blue line represents total number of MXD series.

using the three different methodological approaches detailed above, 24 regional reconstructions were developed: 12 using scaling and 12 using regression techniques (Table 1).

Each chronology and the instrumental records were high and low-pass filtered with a 20-yr centred moving average and then correlated to assess the similarity at high and low frequencies, respectively. Calibration/verification tests against the overlapping T_{MJJAS} regional instrumental temperature record were performed in split periods (Snee, 1977). The tree-ring model was calibrated against the first half of the instrumental temperature record (1900–1952 AD) and validated against the second half (1953–2005 AD), and vice-versa. Quality control statistics such as the coefficient of determination (r^2), Pearson's correlation coefficient between observed and predicted values ($r_{obs-pred}$) and the reduction of error (RE; Cook et al., 1994) were calculated to test the validity of the reconstructions, derived using both methodologies. Usually, RE values above zero indicate reconstruction skills, but since RE has no lower boundary and no test for its statistical significance exists, it should be interpreted carefully. Reconstruction uncertainties related to the differences of the precursor chronologies and the calibration models used for reconstruction were assessed.

Additionally, the maximum temperature reconstruction for the Pyrenees of Büntgen et al. (2008) (PYR) was modified to be fully comparable to the newly developed set of regional mean temperature reconstructions. The original chronology used in Büntgen et al. (2008) was calibrated against May–September mean temperatures to build a reconstruction called "mPYR".

The resulting set of temperature reconstructions was compared with climate simulations performed with global and regional climate models, spanning the last millennium in the target region.

2.4 Model simulations

The global GCM simulations used here were produced with the ECHO-G (Legutke and Voss, 1999) climate model, consisting of the ECHAM4 atmospheric component and the HOPE-G ocean model. ECHAM4 is used with a T30 horizontal resolution (ca. 3.75° lat × long) and HOPE-G with

a horizontal resolution of approx. 2.8° lat × long, with a finer resolution in the tropics increasing towards the Equator where it reaches a minimum meridional grid point separation of 0.5°. The model is run using flux adjustments to avoid climate drift. This work makes use of two existing model simulations (Erik1 and Erik2) produced by driving the model with estimations of the evolution of some natural and anthropogenic forcings during the last millennium. Both simulations were produced starting from different initial conditions and driven by identical forcings from year 1000 AD onwards. Erik1 (Erik2) started from a relatively warm (cold) state and was integrated for 100 yr according to the forcing levels of year 1000 AD, with the forcing values then changed yearly according to the prescribed estimates. Erik1 presents warmer values in the first centuries of the simulation. Goosse et al. (2005) and Osborn et al. (2006) suggest that this simulation is unusually warm in comparison with other model simulations due to the warmer initial state. Erik2 shows similar amplitudes in the temperature changes through the last millennium in comparison to other model runs (e.g. Zorita et al., 2007).

The external forcings used as boundary conditions for the simulations include estimations of changes in solar irradiance and the parameterized effect of stratospheric volcanic aerosols, both adapted from Crowley (2000), as well as the concentrations of greenhouse gases (CO_2, CH_4 and N_2O) provided by Etheridge et al. (1996, 1998) and Battle et al. (1996). For a more in-depth description of the simulations and the external forcings applied as well as model details, the reader should refer to Zorita et al. (2005) and González-Rouco et al. (2006, 2009).

The RCM simulations used herein were produced with a climate version of the model MM5, developed by NCAR and the Pennsylvania State University (Dudhia, 1993; Grell et al., 1994). The model domain is double-nested with resolutions of 90 km and 30 km, respectively. The high-resolution domain covers the area of the Iberian Peninsula. Two 1000-yr-long simulations were run. Each simulation (MM5-Erik1 and MM5-Erik2) was produced by driving the MM5 model with boundary conditions obtained from the ECHO-G Erik1 and Erik2 runs, respectively. The boundary conditions are introduced into the outer domain of the MM5 model through a blending area of five grid points at the boundaries. Specifications for the model, simulation experiments and the physics configuration are also provided in Gómez-Navarro et al. (2011, 2012).

3 Results

3.1 Regional Pyrenees MXD chronologies and climate signal

The PCA performed on the set of MXD chronologies reveals that the first principal component (PC1) is dominant and

Table 1. Statistics of the calibration verification for the 24 regional chronologies developed. r indicates correlation between instrumental and predicted May-to-September temperatures (T_{MJJAS}): for the entire period 1900–2005 AD (r); for the entire period in series low-pass filtered with a 20 yr moving average (r_{lf}) and for the correlations for the two periods of the calibrations ($r_{1900-1952}$ and $r_{1953-2005}$, respectively). RE: reduction of error for the two split periods. (**) indicates significant correlation at 99 % level.

| Regional chronology type | Regional reconstruction code | r | r_{lf} | Split period | | | |
				$r_{(1900-1952)}$	$r_{(1953-2005)}$	RE1	RE2
Regression	**Chrono**						
	RCS_chrono_R	0.36**	−0,19	0.75**	0.54**	−0.70	−0,80
	RCSPT_chrono_R	0.37**	−0.18	0.74**	0.55**	−0.82	−0.94
	300sp_chrono_R	0.59**	0.25	0.75**	0.72**	−0.12	−0.37
	300spPT_chrono_R	0.59**	0.25	0.72**	0.72**	−0.02	−0.43
	Mean						
	RCS_mean_R	0.70**	0.45	0.73**	0.81**	0.09	0.42
	RCSPT_mean_R	0.72**	0.49	0.73**	0.82**	0.21	0.43
	300sp_mean_R	0.60**	0.20	0.73**	0.74**	−0.24	0.12
	300spPT_mean_R	0.61**	0.22	0.74**	0.74**	−0.29	0.00
	Nested PCs						
	PCs_RCS_R	0.73**	0.56	0.81**	0.76**	0.59	0.67
	PCs_RCSPT_R	0.80**	0.58	0.81**	0.84**	0.73	0.68
	PCs_300sp_R	0.67**	0.43	0.81**	0.70**	0.51	0.65
	PCs_300spPT_R	0.68**	0.45	0.81**	0.70**	0.51	0.66
Scaling	**Chrono**						
	RCS_chrono_S	0.36**	−0.19	0.75**	0.54**	−0.04	−4.20
	RCSPT_chrono_S	0.37**	−0.18	0.75**	0.55**	−0.02	−3.95
	300sp_chrono_S	0.59**	0.25	0.75**	0.72**	0.22	0.38
	300spPT_chrono_S	0.59**	0.25	0.72**	0.72**	0.21	0.44
	Mean						
	RCS_mean_S	0.71**	0.45	0.73**	0.81**	0.36	0.69
	RCSPT_mean_S	0.72**	0.49	0.73**	0.82**	0.36	0.66
	300sp_mean_S	0.60**	0.20	0.73**	0.74**	0.36	0.40
	300spPT_mean_S	0.61**	0.22	0.74**	0.74**	0.28	0.47
	Nested PCs						
	PCs_RCS_S	0.71**	0.64	0.73**	0.83**	0.65	0.62
	PCs_RCSPT_S	0.72**	0.78	0.73**	0.84**	0.66	0.62
	PCs_300sp_S	0.66**	0.53	0.73**	0.76**	0.46	0.62
	PCs_300spPT_S	0.66**	0.55	0.74**	0.77**	0.48	0.61
	mPYR	0.62**	0.61	0.57**	0.74**	0.47	−0.85

captures on average 60 % of the variance (Fig. 3). The high percentage of variance explained by PC1 shows slight variations across the different PCA runs, displaying higher percentages of explained variance for PCAs containing a smaller number of MXD chronologies (run1, run2, and from run21 to run25). The leading PC derived from chronologies standardized with 300sp and 300spPT, rather than with RCS or RCSPT, also explains slightly more common variance, although the difference is very small. The first empirical orthogonal function (EOF) describes a coherent spatial pattern of the signal regardless of the standardization method used (Fig. 4). The individual points (MXD chronologies) present the same sign and similar magnitude in the maps of the first EOF for each of the four standardization methods. This suggests that spatially coherent modes of tree-ring variation exist, which may reflect regional-scale modes of climate parameters driving tree growth. The second and subsequent PCA modes, which are similar regardless of the standardization method

used, become less spatially and seasonally coherent, with the sign and magnitude of the relationship, occasionally differing between individual points, likely in response to local or site influences.

The leading mode (PC1) shows high correlations with the seasonal May-to-September temperature and has positive loadings across all the Pyrenees sites (Fig. 5). The highest correlations with climate are for the PC that includes the highest number of MXD chronologies (i.e. run4 and run5) and decreasing with decreasing number of series. The small differences observed in the variance captured by PC1 among the different standardization methods do not have a significant effect on the correlation between PC1 with May-to September-temperature (T_{MJJAS}). The coefficients among the different standardization methods are almost identical. In summary, the mean correlation of PC1 and T_{MJJAS} is 0.64, and it is slightly higher for the standardization method RCS
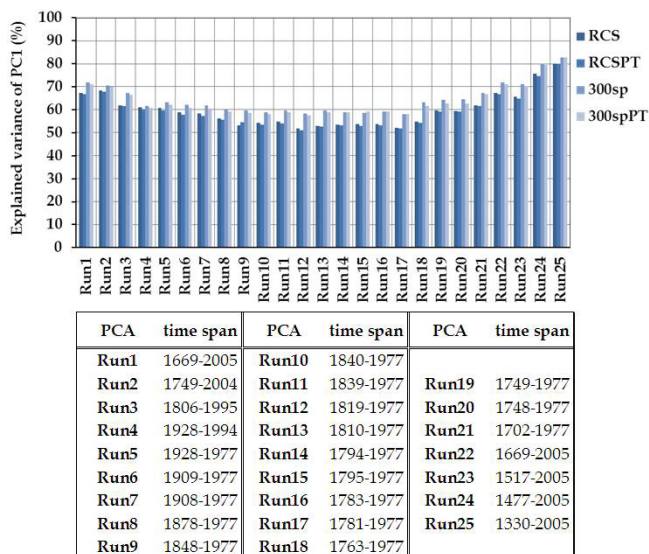
Fig. 3. Variance explained by the PC1 for each PCA run (1 to 25) and for each standardization method (RCS, RCSPT, 300sp, 300spPT). Time span for each PCA is shown in the table.

and RCSPT (mean $r = 0.65$) than for 300sp and 300spPT (mean $r = 0.63$).

The regional chronologies computed as arithmetic means of the 22 MXD site chronologies ("mean") display generally higher correlations with T_{MJJAS}, when the standardization methods RCS and RCSPT (RCS_mean and RCSPT_mean respectively) were used rather than 300sp and 300spPT (300sp_mean and 300sp_mean respectively) (Fig. 5). In comparison to the dominant mode of PCA, only the PC1s of run4 and run5 display larger correlation coefficients (mean $r = 0.78$ and mean $r = 0.76$, respectively) than the RCS_mean and RCSPT_mean ($r = 0.71$ and $r = 0.72$, respectively). In contrast, among the regional series computed as single chronologies ("chrono"), RCS_chrono and RCSPT_chrono overall display the lowest correlations with T_{MJJAS} (below 0.4), while 300sp_chrono and 300spPT_chrono show coefficients of a similar order of magnitude to those displayed by the PCs.

3.2 May-to-September regional reconstruction: scaling and regression

A total of 24 regional reconstructions for the Pyrenees were developed using both scaling and regression techniques applied to each of the 12 regional chronologies developed. The correlations between the reconstructions based on nested PCs and the instrumental T_{MJJAS} record are high for both high (<20 yr) and low-frequency (>20 yr) variations (Table 1). In contrast, the correlations of reconstructions from the group "chrono" are low and they reveal diverging low-frequency information when using RCS and RCSPT as standardization methods (RCS_chrono_R, RCSPT_chrono_R,

RCS_chrono_S, RCSPT_chrono_S). Reconstructions based on "mean" regional chronologies display high correlations with the instrumental T_{MJJAS}; however, the correlations are slightly lower in the low frequency domain compared to the reconstructions based on nested PCs, similarly to the mPYR.

The calibration verification test conducted against the target T_{MJJAS} in two periods (1900–1952 AD; 1953–2005 AD) generally shows a coherent relationship between observed and predicted values for the 24 regional reconstructions; however, large differences in the reduction of error statistic (RE) appear (Table 1). Regional chronologies based on nested PCs display high correlation coefficients in the two calibration periods: both regression-calibrated ($r_{1900-1952} = 0.81$ and $r_{1953-2005} = 0.75$ on average) and scaling-calibrated ($r_{1900-1952} = 0.73$ and $r_{1953-2005} = 0.80$ on average). Similarly, REs are also high (well above 0) for the two verifications. In contrast, even though correlation values are fairly high for the two periods, RE values decline to large negative values when the reconstructed values are obtained by linear regression of single regional chronologies, especially reconstructions from the group "chrono". Single regional chronologies computed as means display higher RE values when the reconstruction is performed using scaling rather than regression (RCS_mean_S, RCSPT_mean_S, 300sp_mean_S, 300spPT_mean_S), The set of reconstructions based on RCS_chrono and RCSPT_chrono displays RE values lower than zero regardless of the technique used for the reconstructions.

The set of May-to-September temperature reconstructions (T_{MJJAS}) spans the period from 1260 to 2006 AD. While most of the reconstructions display no clear long-term trend, the reconstructions RCSPT_chrono_S, RCS_chrono_S and mPYR clearly show an increasing trend starting in 1260 and lasting until around 1850 AD (Fig. 6). Despite this difference regarding the trends, all reconstructions display similar intermediate to low-frequency variations (multi-decadal to centennial time scales), which are, however, less visible in the case of RCSPT_chrono_R and RCS_chrono_R due to their reduced amplitude of the variations. Periods with persistent climate anomalies such as the Medieval Climate Anomaly (Bradley, 2003) and the Little Ice Age (Fagan, 2000) are not pronounced in the set of reconstructions. However, interdecadal variations clearly register the cold periods coincident with solar grand minima, such as those of Dalton (1800–1830 AD), Maunder (1680–1715 AD), Spörer (1480–1520 AD) and Wolf (1340–1380 AD) (Bard et al., 2000). In addition, a minimum in the modern age between 1950 and 1980 AD is shown by all 25 reconstructions including the mPYR. On the other hand, conspicuous maxima also appear during 1300–1330, 1360–1460 and 1710–1740 AD.

The total amplitudes of the 24 reconstructions and the mPYR range from the largest amplitude of RCSPT_mean_S (from -2.49 to $+0.59\,°C$) to the smallest of PCs_300sp_R (from -0.32 to $+0.39\,°C$) at interdecadal time scales. Similarly, changes in the amplitude of variations do not differ
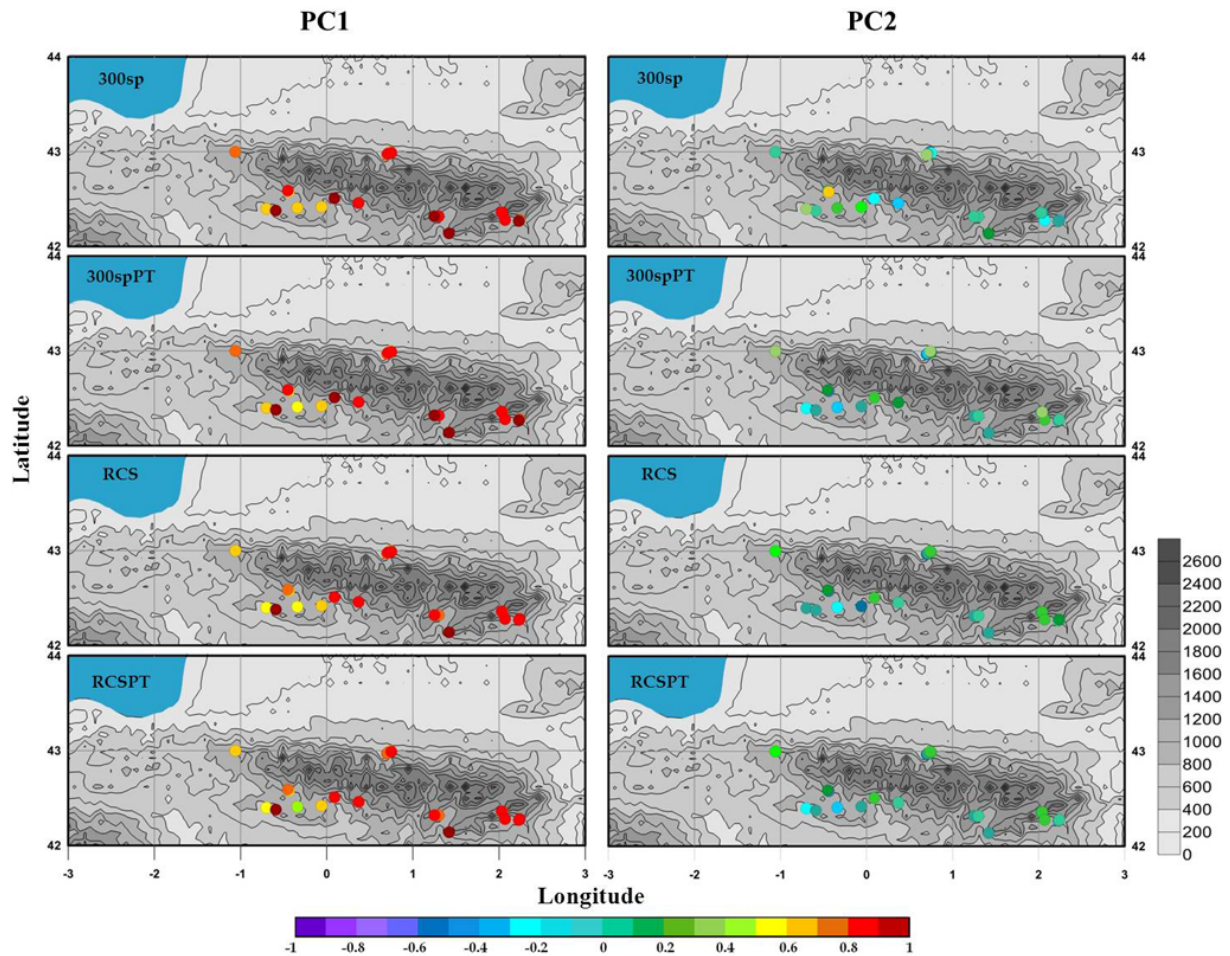
Fig. 4. EOF maps corresponding to the first (PC1) and second (PC2) principal component for each of the standardization methods used for building the site MXD chronologies: 300sp, 300spPT, RCS and RCSPT. The principal component analysis (PCA) was run for the common period 1928–1977 AD.

much if only the preindustrial period is considered (1260–1900 AD).

3.3 Cross-comparison of model simulation and proxy-based climate reconstructions

For the calibration period (1900–1990 AD), the two global (Erik1 and Erik2) and the regional MM5-Erik2 simulations display a marked positive trend in agreement with the instrumental series (Fig. 7). The global simulations display a mean increase of about +1 °C in this period, while for the regional models this increase is less pronounced, i.e. +0.4 °C for MM5-Erik1 and +0.7 °C for MM5-Erik2. The instrumental record displays an increase of approximately +0.7 °C for the same period. However, a pronounced negative temperature anomaly is exhibited in the later part of the 20th century, which is only reproduced by the regional simulation MM5-Erik1.

On the other hand, model simulations and proxy reconstructions disagree to some extent on the magnitude of the warming trend over the 20th century (1900–1990 AD) (Fig. 7). The reconstructions, including mPYR, mostly display negative trends over the same period, ranging from −1 °C (RCS_chrono_S) to −0.1 °C (PCs_RCS_S; PCs_RCSPT_S). Some reconstructions show trends close to zero (PCs_RCS_R; PCs_300sp_R; PCs_300sp_R), and only PCs_RCSPT_R displays a minor increase (+0.05 °C).

When comparing the full length of global and regional simulations and the collection of May-to-September temperature reconstructions, the large interdecadal changes are in agreement (Fig. 7b). A high synchrony is found among the simulations and the tree-ring based reconstructions in periods with large negative temperature anomalies observed at the end of the 18th century, during the Dalton and Spörer solar grand minima, and during periods of positive anomalies as well, e.g. during the middle of the 15th century, the middle to end of the 16th century and during the middle of
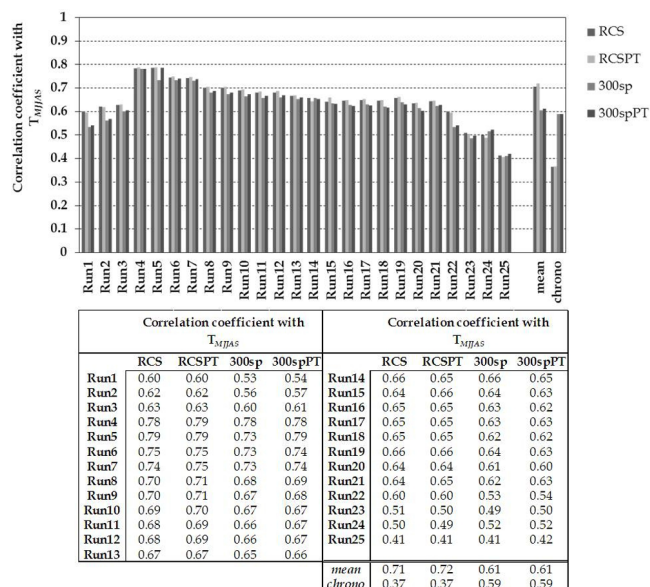
Fig. 5. Pearson's correlation coefficient of the PC1 of each PCA run (1 to 25) and the regional chronologies "mean" and "chrono" and May-to-September mean temperature (T_{MJJAS}) for each standardization method (RCS, RCSPT, 300sp, 300spPT).

the 18th century. Some simulations lack pronounced negative periods such as the Late Maunder solar minimum, which are present in the reconstructions. The simulations Erik1 and MM5-Erik1 display identical periods of negative anomalies corresponding to the Maunder solar minimum, in agreement with the negative anomalies displayed by the set of reconstructions. In the simulations Erik2 and MM5-Erik2, this negative period is delayed.

The largest amplitude of the past temperature variations at interdecadal time scales during the total study period 1260–1990 AD (Fig. 7c) is identified for MM5-Erik2 (from −1.8 to +0.5 °C), among the simulations, and for RCSPT_chrono_S (from −2.49 to +0.6 °C), among the reconstructions. However, the amplitude of the model simulations is generally larger (mean ranging from −1.59 to +0.55 °C) than the amplitude of the reconstructions (mean ranging from −0.83 to +0.43 °C).

If only pre-industrial interdecadal temperature variations (1260–1900 AD) are considered, the model simulations display a mean range of amplitudes from −1.6 to −0.07 °C, while for the set of temperature reconstructions the amplitude ranges from −0.81 to +0.38 °C. In this case, MM5-Erik1 now displays the largest amplitude among the model simulations (from −1.7 to +0.2 °C), while for the set of reconstructions RCSPT_chrono_S still displays the largest amplitude (from −2.49 to +0.6 °C).

4 Discussion

How the individual chronologies should be standardized while preserving as much climate information as possible and how they should be aggregated into regional composites to reduce local influences are key challenges in dendroclimatology. In the context of low frequency preservation, the RCS has been suggested as an alternative to the more traditional standardization procedures such as 300-yr splines or negative exponential functions (Esper et al., 2003). RCS does not preserve decadal or annual frequencies with better efficiency than other techniques (Bunn et al., 2004), but it is assumed to retain more low frequency variability (Esper et al., 2002, 2004).

On the other hand, the development of regional reconstructions from a set of several individual chronologies (from the same and/or different variables) has so far been achieved by PCA (Peters et al., 1981; Enright, 1984; D'Arrigo et al., 1999), arithmetic means (Briffa et al., 2004; Tang et al., 2009) or regional chronologies compiled into a single dataset including all the individual measurements (Esper et al., 2007; Büntgen et al., 2008).

The standardization techniques used in the present study have contributed to visible differences among various reconstructions, as reported by other authors (Esper et al., 2002; Helama et al., 2004). However, our results suggest that these differences may be enhanced when deriving a regional chronology from the individual series rather than by aggregation of the individual site chronologies. Hence, we could not find large differences among regional reconstructions when they were calculated as an average of the 22 MXD site chronologies ("mean") or when using nested PCs (PCs), regardless of the standardization procedures (300-yr spline or RCS, with or without PT) applied to the individual chronologies. Differences due to the standardization arose in the regional reconstructions, which were derived from regional chronologies computed as a single chronology including all 804 individual series in one run (the group named "chrono"). Within this group, regional chronologies standardized using RCS (RCSPT_chrono and RCS_chrono) display the largest differences, whereas chronologies standardized with a 300-yr spline (300spPT_chrono and 300sp_chrono) produced results more similar to the results of the "mean" and "PCs" regional chronologies.

Correlations between T_{MJJAS} and RCS_chrono and RCSPT_chrono are consistently lower compared to the correlations displayed by other regional chronologies, pointing to a less well-preserved climate signal. Furthermore, the resulting reconstructions based on these regional chronologies display either a pronounced positive trend spanning the entire series lengths (RCSPT_chrono_S and RCS_chrono_S) or an extremely reduced amplitude of past climate variations (RCSPT_chrono_R and RCS_chrono_R). Similarly, PYR and mPYR are also based on a regional chronology computed using RCS and display similar but less pronounced positive
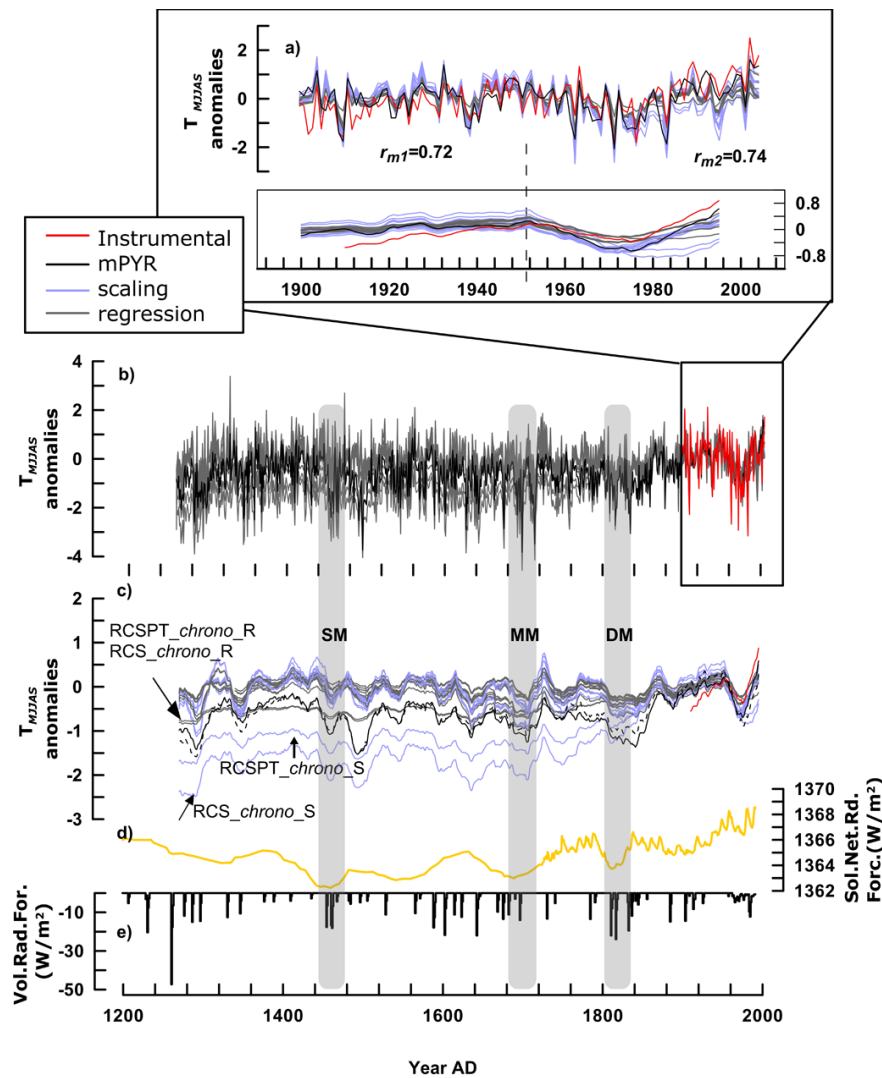
Fig. 6. May-to-September mean temperature (T_{MJJAS}) reconstructions. **(a)** Calibration-verification for the 24 different regional reconstructions performed by regression (grey lines) and scaling (blue lines), the mPYR (black line) and the instrumental T_{MJJAS} record (red line). The bottom panel displays low-pass filtered series (20 yr moving average). Mean correlations (r_m) for the two split periods (1900–1952 and 1953–2005 AD) are also shown; **(b)** comparison between the instrumental series, the 24 Pyrenees regional reconstructions and mPYR for the entire reliable period; **(c)** 20 yr low-pass filtered reconstructions and instrumental record. The dashed black line represents the original May-to-September maximum temperature reconstruction from Büntgen et al. (2008) (PYR); **(d–e)** solar and volcanic forcing derived from Crowley (2000) and used to drive the climate models. Shaded areas indicate periods with solar grand minima: Dalton minimum (DM), Maunder minimum (MM) and Spörer minimum (SP).

trend. These trends are in disagreement with all other newly developed reconstructions, including the reconstructions derived from 300sp_chrono and 300spPT_chrono.

Therefore, it becomes obvious that the differences stem from the computation of the regional chronology, not only by using a single file merging all the individual measurements together, but also from the application of the RCS as the standardization method.

RCS requires sampling loads structured in age classes with similar replication (Esper et al., 2002), which limits its application in practice. The set of samples from the Pyrenees, as

well as the set used for PYR and mPYR, does not seem to adequately fulfil the RCS requirements: the sample depth diagram shows an extremely high number of samples concentrated in the most recent period (from 1800 to 2005 AD, approximately), whereas the replication in the rest of the period (from 1260 to 1800 AD) is much lower. Such anomalously high and low replications can introduce a bias into the final chronology (Cook and Peters, 1997; Esper et al., 2003; Helama et al., 2004) and therefore in the resulting reconstruction. Thus, it seems likely that the trend of RCSPT_chrono_S and RCS_chrono_S may be an artefact due to a suboptimal
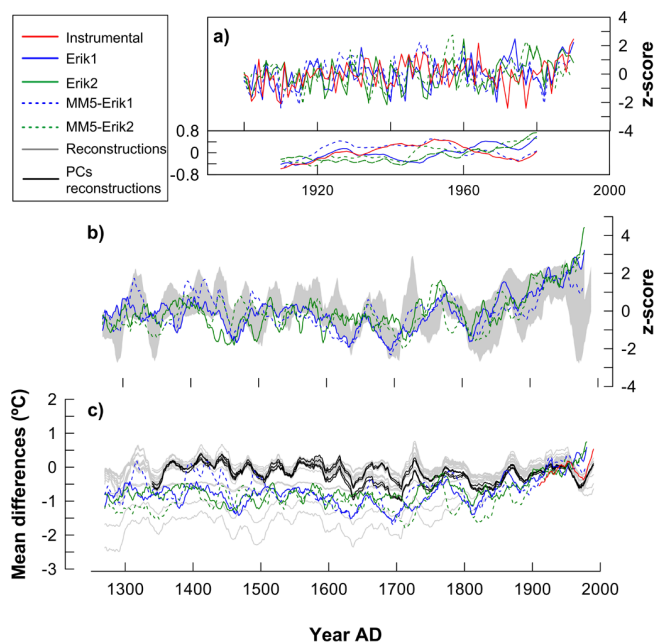
Fig. 7. Comparison of reconstructed and simulated May-to-September mean temperature (T_{MJJAS}) for the last 750 yr. Grey lines/shade correspond to the range of the 24 MXD-based temperature reconstructions developed at the Pyrenees. Coloured lines correspond to the different model outputs: Erik1 (blue), Erik2 (green), MM5-Erik1 (dashed blue) and MM5-Erik2 (dashed green). **(a)** Comparison of the simulated and the instrumental T_{MJJAS} record (red line). **(b)** Series scaled to mean 0 and standard deviation 1. **(c)** Series in anomalies (differences from reference period 1900–2005 AD). Black series correspond to the reconstructions PCs_RCS_S, PCs_RCSPT_S, PCs_300sp_S and PCs_300spPT_S. All series smoothed with a 20 yr centred moving average (except for the upper half of panel **a**).

dataset used for the regional chronology constructed using RCS. Such a trend was removed in the case of RCSPT_chrono_R and RCS_chrono_R due to their poor calibration, which led to a subsequent underestimation of the variability imparted by the regression technique, and to reconstructions with reduced amplitude (Cook et al., 1994).

Based on the calibration verification tests, regional reconstructions derived from nested PCs performed better than others, regardless of the standardization procedure applied to the individual chronologies, or irrespective of the reconstruction technique used, which indicates that this approach emphasizes the leading mode of co-variation between the tree-ring series (Peters et al., 1981). The amplitudes of our reconstructions are also larger when performed with scaling than with regression; however, the RE values become low or negative due to inflated error estimates, as previously reported by Esper et al. (2005b) and McCarrol et al. (2011). However, for series with generally good calibration, the RE values were similar for the reconstructions based on scaling as well as on regression. Thus, differences in RE between

both reconstruction techniques are reduced, as the proxy better records the climate signal.

Despite showing high correlations with the instrumental record at low frequencies, the 24 regional reconstructions and the mPYR graphically display general overestimations of past temperatures until 1940 and underestimations from 1980 AD onwards. This systematic misfit between instrumental measurements and proxy estimates has been previously described and the possible causes discussed (Frank et al., 2007). The tree-ring data from the Pyrenees display a strong and stable relationship with temperature, and therefore, a loss of tree sensitivity to climate seems unlikely ("the divergence problem"; Briffa et al., 1998; D'Arrigo et al., 2008). Thus, this mismatch may be due to the effect of the standardization methods on the low-frequency climate information encoded in tree-ring series (Cook et al., 1995; Esper et al., 2002) or alternatively related to the instrumental data used for calibration (Frank et al., 2007; Esper et al., 2005b, 2010). The selected instrumental data for the Pyrenees and the homogenization and adjustments applied to these data also have a determinant effect on the resulting proxy-based reconstructions (Frank et al., 2007). In our case, no clear conclusion can be drawn without further specific work directed to answer this particular question.

The comparison between the output of the model simulations and the range established by the different reconstructions shows synchronized variability at the multi-decadal time scales. This synchronism indicates that the external forcings applied to the model efficiently reproduce the timing of the main periods of anomalous past temperature variations in the Pyrenees region. Indeed, the spread among the four simulated temperatures is mostly within the range estimated from the different standardization and reconstruction methods applied over the last 750 yr. These results confirm that past multi-decadal temperature variations in this region are driven to a great extent by solar activity and volcanic eruptions.

Model simulations, however, also show some clear discrepancies in comparison to the tree-ring based reconstructions, such as the duration and magnitude of warming or cooling events of particular climatic episodes (e.g. in the 15th and 16th century). A likely reason for such differences is that at higher frequencies, i.e. decadal time scales, the agreement between model simulations and reconstructions is lower, because the climate variability at these time scales is mostly internal and not driven by the external forcing (Zorita et al., 2007; Gómez-Navarro et al., 2012).

However, the most relevant differences between the model simulations and proxy-based reconstructions are the positive trends from 1850 AD–present displayed by the simulations but not reproduced by the reconstructions, and the differences in reproducing temperature variability within the 20th century.

On the one hand, the positive trend shown by the simulations is likely due to the external forcings prescribed. The

increasing trends in regional and global temperatures described by the simulations may be ascribed to the increase in solar irradiance and greenhouse gas forcing. However, since the model runs incorporate both natural and anthropogenic forcings, it is difficult to distinguish the effect of the individual forcings in the resulting simulation and especially in the resulting trend. Thus, it is not possible to know whether the observed difference between these simulations and reconstructions is due to an underestimation by the proxy-based reconstructions or to an overestimation by the models.

On the other hand, instrumental series and proxy-based reconstructions show a pronounced cooling from 1950 until approximately 1980 AD, which does not agree with the increasing warming trend replicated by simulations for the second part of the 20th century. It is important to note that cooling factors, such as aerosols and land-use or vegetation changes (Hansen et al., 2002; Betts et al., 2007), are not included as external forcing in the simulations. The Pyrenees range has experienced an increase of forest coverage of about 15 % since the 1950s until present due to land-use changes (Garcia-Ruiz and Lasanta, 1990) and because of reforestation politics (Ortigosa et al., 1990). Deforestation increases surface albedo, which may result in a cooling effect (Betts et al., 2007). After the minimum, the progressive increase in forest coverage may produce a reduction in albedo, and thus may have contributed to the increase in temperatures observed from mid-1970s onwards.

Aerosols in the troposphere also tend to produce surface cooling since they intercept incoming sunlight and reduce the energy flux arriving to the surface (Charlson et al., 1992). In addition to this direct effect, there are several "indirect", cloud-mediated effects of aerosols, which all result in cooling (Andreae et al., 2005), although its magnitude is still very uncertain. Whether land-use changes or aerosols or a combination of both can produce the observed negative temperature anomaly in the second half of the 20th century remains open to discussion, since their role in surface temperatures in this region is not well-known. Further simulations, combining different kinds of forcings and taking into account explicitly the increase in aerosols and land-use changes during the industrial era (i.e. Jungclaus et al., 2010), which are not considered here, could elucidate this uncertainty.

Finally, although internal variability can be claimed to be responsible for part of these differences, the analysis of two regional simulations, both driven by the same forcing used here, indicates that the role of internal variability in the long-term trends of the simulated surface temperature over the Iberian Peninsula is small (Gómez-Navarro et al., 2012). However, this does not rule out that the real internal variability, which is part of the observed record, may indeed explain part of the mismatch. Thus, it may also be possible that the described regional cooling is just due to internal variability without the need to involve vegetation changes or aerosol forcing.

Based on the differences in trend and magnitude of the 20th century warming described above, it is not surprising that, if we consider the whole common period (1260–1990 AD), the amplitudes of the temperature variations are considerably larger in the model simulations than in the most reliable reconstructions. If the 20th century is not considered, the amplitude of the annual temperature variations is still wider for the model simulations, but the differences with the tree-ring based reconstructions are reduced. It is worth mentioning that, among the model simulations, the finer resolution of regional models seems to enhance the interdecadal amplitude of the temperature variations.

5 Conclusions

We provide a set of newly developed May-to-September mean temperature reconstructions for the Pyrenees that represent an improvement in comparison to the reconstruction by Büntgen et al. (2008), although our reconstructions still do not perfectly match the low-frequency variations of the instrumental record. Similarities between the interdecadal temperature variations obtained for reconstruction variants indicate the good performance of all standardization procedures for retaining inter-annual to interdecadal climate information. However, when the regionally representative tree-ring series are constructed as a single chronology (including all single measurements into a single file) and standardized with the RCS method, unreliable results may be obtained if the requirements of the RCS method regarding sample replication and age categorization are not fulfilled. Overall, nested PCs have demonstrated to be the most appropriate approach to build a regional chronology based on a set of local chronologies, regardless of the standardization procedure used for the individual site chronologies. Additionally, no large differences were found between reconstruction techniques (scaling and regression) when using chronologies based on nested PCs. Thus, the quality of the final reconstruction seems to depend more on the standardization performed and the method applied to construct the regional chronology, rather than on the reconstruction method employed.

On the other hand, the good agreements on interdecadal scales between tree-ring based reconstructions and global and regional model simulations point to the combination of solar variability and volcanic activity as the main factors driving summer temperature variations over the last millennium in the Pyrenees. As we have developed regional reconstructions, it is difficult to conclude whether the more realistic topography and land-use categories of the regional model would yield a more accurate replication of temperature variations at local scales. However, the regional model seems to yield larger amplitudes of temperature variations compared to the global models. This is expected because variability is subdued when larger spatial averaging is applied.

Cooling factors, such as aerosols and vegetation changes, are not included as external forcings in the simulations, and their potential contributions to the changes in the surface temperatures in this region are still unclear. Thus, the mismatch in the 20th century between the simulations and the observations discussed here could be related to shortcomings in the models, in the external forcings used to drive these simulations, or in both. Further simulations from the same area, including aerosols and land use changes as external forcings, could help to solve some of the questions that remain unanswered. This analysis will be addressed in future studies

Supplementary material related to this article is available online at: http://www.clim-past.net/8/919/2012/ cp-8-919-2012-supplement.pdf.

References

Agustí-Panareda, A., Thompson, R., and Livingstone, D. M.: Reconstructing temperature variations at high elevation lake sites in Europe during the instrumental period, Verh. Int. Ver. Limn., 27, 479–483, 2000.

Andreae, M. O., Jones, C. D., and Cox, P. M.: Strong present-day aerosol cooling implies a hot future, Nature, 435, 1187–1190, doi:10.1038/nature03671, 2005.

Bard, E., Raisbeck, G., Yiou, F., and Jouzel, J.: Solar irradiance during the last 1200 years based on cosmogenic nuclides, Tellus B, 52, 985–992, 2000.

Battle, M., Bender, M., Sowers, T., Tans, P. P., Butler, J. H., Elkins, J. W., Ellis, J. T., Conway, T., Zhang, N., Lang, P., and Clarke, A. D.: Atmospheric gas concentrations over the past century measured in air from firn and the South Pole, Nature, 383, 231–235, 1996.

Betts, R. A., Falloon, P. D., Goldewijk, K. K., and Ramankutty, N.: Biogeophysical effects of land use on climate: Model simulations of radiative forcing and large-scale temperature change, Agr. Forest Meteorol., 142, 216–233, 2007.

Bradley, R. S., Hughes, M. K., and Diaz, H. F.: Climate in Medieval Time, Science, 302, 404–405, doi:10.1126/science.1090372, 2003.

Briffa, K. R. and Melvin, T. M.: A closer look at Regional Curve Standardisation of tree-ring records: justification of the need, a warning of some pitfalls, and suggested improvements in its application, in: Dendroclimatology: Progress and Prospects, edited

by: Hughes, M. K., Diaz, H. F., and Swetnam, T. W., Springer Verlag, 2008.

Briffa, K. R., Schweingruber, F., Jones, P., and Osborn, T.: Reduced sensitivity of recent tree growth to temperature at high northern latitudes, Nature, 391, 678–682, 1998.

Briffa, K. R., Osborn, T. J., Schweingruber, F. H., Jones, P. D., Shiyatov, S. G., and Vaganov, E. A.: Tree-ring width and density data around the Northern Hemisphere: part 1, local and regional climate signals, Holocene, 12, 737–757, 2002.

Briffa, K. R., Osborn, T. J., and Schweingruber, F. H.: Large-scale temperature inferences from tree rings: a review, Global Planet. Change, 40, 11–26, 2004.

Brunet, M., Jones, P. D., Sigro, J., Saladie, O., Aguilar, E., Moberg, A., Della-Marta, P. M., Lister, D., Walther, A., and Lopez, D.: Temporal and spatial temperature variability and change over Spain during 1850–2005, J. Geophys. Res-Atmos., 112, D12117, doi:10.1029/2006JD008249, 2007.

Brunet, M., Saladié, O., Jones, P., Sigró, J., Aguilar, E., Moberg, A., Lister, D., Walther, A., and Almarza, C.: A case-study/guidance on the development of long-term daily adjusted temperature datasets, World Meteorological Organization WCDMP-66/ WMO-TD-1425, Geneva, 44 pp., 2008.

Büntgen, U., Frank, D. C., Nievergelt, D., and Esper, J.: Summer temperature variations in the European Alps, AD 755–2004, J. Climate, 19, 5606–5623, 2006.

Büntgen, U., Frank, D. C., Kaczka, R. J., Verstege, A., Zwijacz-Kozica, T., and Esper, J.: Growth/climate response of a multi-species tree-ring network in the Western Carpathian Tatra Mountains, Poland and Slovakia, Tree Physiol., 27, 689–702, 2007.

Büntgen, U., Frank, D. C., Grudd, H., and Esper, J.: Long-term summer temperature variations in the Pyrenees, Clim. Dynam., 31, 615–631, 2008.

Büntgen, U., Frank, D. C., Trouet, V., and Esper, J.: Diverse climate sensitivity of Mediterranean tree-ring width and density, Trees-Struct. Funct., 24, 261–273, 2010.

Bunn, A. G., Sharac, T. J., and Graumlich, L. J.: Using a simulation model to compare methods of tree-ring detrending and to investigate the detectability of low-frequency signals, J. Tree-Ring Res., 60, 77–90, 2004.

Charlson, R. J., Schwartz, S. E., Hales, J. M., Cess, R. D., Coakley Jr., J. A., Hansen, J. E., and Hoffman, D. J.: Climate forcing by anthropogenic aerosols, Science, 255, 423–430, doi:10.1126/science.255.5043.423, 1992.

Collins, W. D., Rasch, P. J., Eaton, B., Fillmore, D. W., Kiehl, J., Beck, T. C., and Zender, C.: Simulation of Aerosol Distributions and Radiative Forcing for INDOEX: Regional Climate Impacts, J. Geophys. Res., 107, 8028, doi:10.1029/2000JD000032, 2002.

Cook, E. R. and Holmes, R. L.: Program ARSTAN, Version 1, 72 pp., 1986.

Cook, E. R. and Kairiukstis, L. A.: Methods of dendrochronology: applications in the environmental sciences, International Institute for Applied Systems Analysis, Boston, MA, USA, Kluwer Academic Publishers, 1990.

Cook, E. R. and Peters, K.: Calculating unbiased tree-ring indices for the study of climatic and environmental change, Holocene, 7, 361–370, 1997.

Cook, E. R., Briffa, K. R., and Jones, P. D.: Spatial regression methods in dendroclimatology: A review and comparison of two techniques, Int. J. Climatol., 14, 379–402, 1994.

Cook, E. R., Briffa, K. R., Meko, D. M., Graybill, D. A., and Funkhouser, G.: The segment length curse in long tree-ring chronology development for paleoclimatic studies, Holocene, 5, 229–237, 1995.

Crowley, T. J.: Causes of climate change over the past 1000 years, Science, 289, 270–277, 2000.

D'Arrigo, R., Gordon, C. J., Free, M., and Robock, A.: Northern Hemisphere annual to decadal temperature variability for the past three centuries: Tree-ring and model estimates, Climatic Change, 42, 663–675, 1999.

D'Arrigo, R., Wilson, R., Liepert, B., and Cherubini, P.: On the "Divergence Problem" in Northern Forests: A Review of the Tree-Ring Evidence and Possible Causes, Global Planet. Change, 60, 289–305, 2008.

Dudhia, J.: A nonhydrostatic version of the Penn StateNCAR mesoscale model: Validation tests and simulation of an Atlantic cyclone and cold front, Mon. Weather Rev., 121, 1493–1513, 1993.

Enright, N. J.: Principal components analysis of tree-ring/climate relationships in white spruce (Picea glauca) from Schefferville, Canada. J. Biogeogr., 11, 353–361, 1984.

Esper, J., Cook, E. R., and Schweingruber, F. H.: Low-frequency signals in long tree-ring chronologies and the reconstruction of past temperature variability, Science, 295, 2250–2253, 2002.

Esper, J., Cook, E. R., Krusic, P. J., Peters, K., and Schweingruber, F. H.: Tests of the RCS method for preserving low-frequency variability in long tree-ring chronologies, Tree-Ring Res., 59, 81–98, 2003.

Esper, J., Frank, D. C., and Wilson, R. J. S.: Climate reconstructions: low frequency ambition and high frequency ratification, Eos Trans. Am. Geophys. Union, 85, 113–130, 2004.

Esper, J., Wilson, R. J. S., Frank, D. C., Moberg, A., Wanner, H., and Luterbacher, J.: Climate: past ranges and future changes, Quaternary Sci. Rev., 24, 2164–2166, 2005a.

Esper, J., Frank, D. F., Wilson, R. J. S., and Briffa, K. R: Effect of scaling and regression on reconstructed temperature amplitude for the past millennium, Geophys. Res. Lett. 32, L07711, doi:10.1029/2004GL021236, 2005b.

Esper, J., Frank, D., Büntgen, U., Verstege, A., Luterbacher, J., and Xoplaki, E.: Long-term drought severity variations in Morocco, Geophys. Res. Lett. 34, L17702, doi:10.1029/2007GL030844, 2007.

Esper, J., Frank, D., Büntgen, U., Verstege, A., Hantemirov, R. M., and Kirdyanov, A.: Trends and uncertainties in Siberian indicators of 20th century warming, Global Chang. Biol., 16, 386–398, 2010.

Etheridge, D., Steele, L. P., Langenfelds, R. L., Francey, R., Barnola, J., and Morgan, V.: Natural and anthropogenic changes in atmospheric CO_2 over the last 1000 years from air in Antarctic ice and firn, J. Geophys. Res., 101, 4115–4128, 1996.

Etheridge, D. M., Steele, L. P., Francey, R. J., and Langenfelds, R. L.: Atmospheric methane between 1000 A.D. and present: Evidence of anthropogenic emissions and climatic variability, J. Geophys. Res., 103(D13), 15979–15993, 1998.

Fagan, B.: The Little ice age: how climate made history, 1300–1850, ISBN 0465022723, 2000.

Frank, D. C., Büntgen, U., Böhm, R., Maugeri, M., and Esper, J.: Warmer early instrumental measurements versus colder reconstructed temperatures: shooting at a moving target, Quaternary

Sci. Rev., 26, 3298–3310, 2007.

Fritts, H. C.: Tree Rings and Climate, Academic Press, New York, 1976.

Garcia-Ruiz, J. M. and Lasanta, T.: Land use changes in the Spanish Pyrenees, Mt. Res. Dev., 10, 201–214, 1990.

Gleckler, P. J., Taylor, K. E., and Doutriaux, C.: Performance metrics for climate models, J. Geophys. Res., 113: D06104, doi:10.1029/2007JD008972, 2008.

Gómez-Navarro, J. J., Montávez, J. P., Jerez, S., Jiménez-Guerrero, P., Lorente-Plazas, R., González-Rouco, J. F., and Zorita, E.: A regional climate simulation over the Iberian Peninsula for the last millennium, Clim. Past, 7, 451–472, doi:10.5194/cp-7-451-2011, 2011.

Gómez-Navarro, J. J., Montávez, J. P., Jiménez-Guerrero, P., Jerez, S., Lorente-Plazas, R., González-Rouco, J. F., and Zorita, E.: Internal and external variability in regional simulations of the Iberian Peninsula climate over the last millennium, Clim. Past, 8, 25–36, doi:10.5194/cp-8-25-2012, 2012.

González-Rouco, J. F., Beltrami, H., Zorita, E., and von Storch, H.: Simulation and inversion of borehole temperature profiles in surrogate climates: Spatial distribution and surface coupling, Geophys. Res. Lett., 33, L024693, doi:10.1029/2001JD001143, 2006.

González-Rouco, J. F., Beltrami, H., Zorita, E., and Stevens, M. B.: Borehole climatology: a discussion based on contributions from climate modeling, Clim. Past, 5, 97–127, doi:10.5194/cp-5-97-2009, 2009.

Goosse, H., Crowley, T. J., Zorita, E., Ammann, C. M., Renssen, H., and Driesschaert, E.: Modelling the climate of the last millennium: what causes the differences between simulations?, Geophys. Res. Lett., 32, L06710, doi:10.1029/2005GL022368, 2005.

Grell, G. A., Dudhia, J., and Stauffer, D. R.: A description of the fifth-generation penn state/ncar mesoscale model (mm5), Technical Report NCAR/TN-398+STR, National Center for Atmospheric Research, 1994.

Grudd, H.: Tornetrask tree-ring width and density AD 500–2004: a test of climatic sensitivity and a new 1500 year reconstruction of northern Fennoscandian summers, Clim. Dynam., 31, 843–857, 2008.

Hansen, J., Sato, M., Nazarenko, L., Ruedy, R., Lacis, A., Koch, D., Tegen, I., Hall, T., Shindell, D., Santer, B., Stone, P., Novakov, T., Thomason, L., Wang, R., Wang, Y., Jacob, D., Hollandsworth, S., Bishop, L., Logan, J., Thompson, A., Stolarski, R., Lean, J., Willson, R., Levitus, S., Antonov, J., Rayner, N., Parker, D., and Christy, J.: Climate forcings in Goddard Institute for Space Studies SI2000 simulations, J. Geophys. Res., 107, 4347, doi:10.1029/2001JD001143, 2002.

Hegerl, G. C., Crowley, T. J., Hyde, W. T., and Frame, D. J.: Climate sensitivity constrained by temperature reconstrcutions over the past seven centuries, Nature, 440, 1029–1032, 2006.

Helama, S., Lindholm, M., Timonen, M., and Eronen, M.: Detection of climate signal in dendrochronological data analysis: A comparison of tree ring standardization methods, Theor. Appl. Climatol., 79, 239–254, 2004.

Holmes R. L.: Computer-assisted quality control in tree-ring dating and measurement, Tree-Ring Bulletin 43, 69–78, 1983.

IPCC: Climate change, fourth assessment report, Cambridge University Press, London, UK, 2007.

Jansen, E., Overpeck, J., Briffa, K. R., Duplessy, J. C., Masson-Delmontte, V., Olago, D., Otto-Bliesner, B., Peltier, W. R., Rahmstorf, S., Ramesh, R., Raynaud, D., Rind, D., Solomina, O., Villalba, R., and Zhang, D.: Paleoclimate, in: Climate Change 2007: The Physical Science Basis, Contribution of Working Group I to the Fourth Assessment Report of the Intergovernmental Panel on Climate Change, edited by: Solomon, S., Qin, D., Manning, M., Chen, Z., Marquis, M., Averyt, K. B., Tignor, M., and Miller, H. L., Cambridge, United Kingdom and New York, NY, USA, Cambridge University Press, 2007.

Jones, P. D., Briffa, K. R., Osborn, T. J., Lough, J. M., van Ommen, T. D., Vinther, B. M., Luterbacher, J., Wahl, E. R., Zwiers, F. W., Mann, M. E., Schmidt, G. A., Ammann, C. M., Buckley, B. M., Cobb, K. M., Esper, J., Goosse, H., Graham, N., Jansen, E., Kiefer, T., Kull, C., Küttel, M., Mosley-Thompson, E., Overpeck, J. T., Riedwyl, N., Schulz, M., Tudhope, A. W., Villalba, R., Wanner, H., Wolff E., and Xoplaki, E.: High-resolution palaeo-climatology of the last millennium: a review of current status and future prospects, Holocene, 19, 3–49, 2009.

Jungclaus, J. H., Lorenz, S. J., Timmreck, C., Reick, C. H., Brovkin, V., Six, K., Segschneider, J., Giorgetta, M. A., Crowley, T. J., Pongratz, J., Krivova, N. A., Vieira, L. E., Solanki, S. K., Klocke, D., Botzet, M., Esch, M., Gayler, V., Haak, H., Raddatz, T. J., Roeckner, E., Schnur, R., Widmann, H., Claussen, M., Stevens, B., and Marotzke, J.: Climate and carbon-cycle variability over the last millennium, Clim. Past, 6, 723–737, doi:10.5194/cp-6-723-2010, 2010.

Legutke, S. and Voss, R.: The Hamburg Atmosphere-Ocean Coupled Circulation Model ECHO-G. Technical report, No 18, German Climate Computer Center (DKRZ), Hamburg, 1999.

Macias, M., Andreu, L., Bosch, O., Camarero, J. J., and Gutiérrez, E.: Increasing aridity is enhancing Silver fir (Abies alba Mill.) water stress in the south-western distribution limit, Climatic Change, 79, 289–313, 2006.

McCarroll, D., Tuovinen, M., Campbell, R., Gagen, M., Grudd, H., Jalkanen, R., Loader, N. J., and Robertson, I.: A critical evaluation of multi-proxy dendroclimatology in northern Finland, J. Quaternary Sci., 26, 7–14, 2011.

Ortigosa, L., Garcia-Ruiz, J. M., and, Gil, E.: Land reclamation by reforestation in the Central Pyrenees, Mt. Res. Dev., 10, 281–288, 1990.

Osborn, T., Raper, S. C. B., and Briffa, K. R.: Simulated climate change during the last 1000 years: comparing the ECHO-G general circulation model with the MAGICC simple climate model, Clim. Dynam., 27, 185–187, doi:10.1007/s00382-006-0129-5, 2006.

Peters, K., Jacoby, G. C., and Cook, E. R.: Principal components analysis of tree-ring sites, Tree-ring Bulletin, 41, 1–19, 1981.

Polge, H.: Study of wood density variations by densitometric analysis of X-ray negative of samples taken with a pressler auger, Paper presented at Meeting of IUFRO Section 41, 1965.

Snee, R. D.: Validation of Regression Models: Models and Examples, Technometrics, 19, 415–428, 1977.

Stokes, M. A. and Smiley, T. L.: Introduction to tree-ring dating, Chicago, IL, USA, University of Chicago Press, 1968.

Tan, M., Shao, X., Liu, J., and Cai, B.: Comparative analysis between a proxy-based climate reconstruction and GCM-based simulation of temperatures over the last millennium in China, J. Quaternary Sci., 24, 547–551, 2009.

Zorita, E., González-Rouco, J. F., von Storch, V., Montávez, J. P., and Valero, F.: Natural and anthropogenic modes of surface temperature variations in the last thousand years, Geophys. Res. Lett., 32, L08707, doi:10.1029/2004GL021563, 2005.

Zorita, E., González-Rouco, F., and von Storch, H.: Comment to "Testing the fidelity of methods used in proxy-based reconstructions of past climate" by Mann et al., J. Climate, 20, 3693–3698 doi:10.1175/JCLI4171.1, 2007.

Zorita, E., Moberg, A., Leijonhufvud, L., Wilson, R., Brazdil, R., Dobrovolny, P., Luterbacher, J., Bohm, R., Pfister, C., Glaser, R., Soderberg, J., and González-Rouco, F.: European temperature records of the past five centuries based on documentary information compared to climate simulations, Climatic Change, 101, 143–168, 2010.